Experimental Investigation of Spatial Pattern Formation in Physical Systems of Activator Inhibitor Type

Hans-Georg Purwins, Christian Radehaus, and Jürgen Berkemeier
Institute for Applied Physics, University of Münster, Münster

Z. Naturforsch. **43a**, 17–29 (1988); received October 10, 1987

We investigate experimentally stationary stable states of activator (w) inhibitor (v) type systems corresponding to the reaction diffusion equation

$$\delta \cdot \dot{v} = \Delta v + w - v; \quad \dot{w} = \sigma \Delta w + f(w) - v; \quad \delta, \quad \sigma = \text{const} > 0$$

with $f(w)$ monotonically increasing for small and decreasing for large $|w|$. We first describe some general mathematical properties and present qualitative results obtained from numerical calculations. We then investigate experimentally electrical networks described by the spatially discretized version of the above equation. Calculation and experiment are in good agreement. We also interprete a two dimensional-network as an equivalent circuit for a composite material consisting of a linear and a nonlinear layer with an s-shaped current density electric field characteristic. This model is used for a phenomenological description of spatial structures and global current voltage characteristics observed experimentally in pin-diode like and gas discharge devices. The model accounts very well for the experimental results obtained so far. It is concluded that the above equation and the corresponding experimental setup are of great interest for fundamental investigations of self controlled processes in nature.

Keywords: Activator Inhibitor System, Reaction Diffusion System, Electrical Network, Semiconductor, Gas Discharge

1. Introduction

In 1952 Turing [1] has shown that nonlinear dynamical systems with identical cells described by two dependent variables and coupled diffusively (elastically) exhibit nontrivial stable stationary structures. Since then the temporal and spatial structures including stability and bifurcation of various systems described by nonlinear ordinary and partial differential reaction diffusion equations have been investigated. A comprehensive treatment of the mathematical aspects of reaction diffusion equations is given by Smoller [2], Fife [3] and Rothe [4]. Examples of applications in biology are given by Murray [5]. Other applications in chemistry, ecology and other sciences are widely spread in the literature; several references can be found in the text of Smoller [2]. Efforts to understand temporal and spatial structures in physical systems by using nonlinear reaction diffusion equations have been concentrated mainly on wave propagation, in particular in the form of solitons [6]. Cases where stationary spatial structures of reaction diffusion systems have been treated are reported e.g. by the Bruxelles school, by Haken, by Gierer, by Schlögl [7], by Schöll [8] and by Kerner and Osipov [9]. In the latter an effort is made to understand current filamentation in nonlinear semiconductor devices. – Interestingly enough there are practically no investigations of chaos in spatially extended systems.

In the present paper we concentrate on stable stationary states of reaction diffusion systems related to the two component activator inhibitor equation

$$\begin{aligned}
\delta v_{t'} &= \Delta v + w - v, & f(0) &= 0,\\
w_{t'} &= \sigma \Delta w + f(w) - v, & f'(0) &= \lambda,\\
v &= v(x, y, t'), & \delta, \sigma, \lambda &\geq 0,\\
w &= w(x, y, t').
\end{aligned} \tag{1}$$

$f(w)$ is assumed to be a monotonically increasing function for small $|w|$ and decreasing for large $|w|$. In its simplest form it can be written as

$$f(w) = \lambda w - w^3. \tag{2}$$

In chemical terms (1) describes the temporal and spatial dependence of the two components v and w. w catalyses the production of itself and of v and is therefore called activator; v inhibits the production of itself and of w and is called inhibitor. The temporal

Reprint requests to Prof. Dr. H.-G. Purwins, Institut für Angewandte Physik, Corrensstraße 2–4, D-4400 Münster.

0932-0784 / 88 / 0100-0017 $ 01.30/0. – Please order a reprint rather than making your own copy.

changes of v and w in a volume element are due to diffusion and chemical reaction. For v the latter are linear whereas for w the autocatalytic reaction with saturation leads to the nonlinear production term $f(w)$. We investigate systems corresponding to (1) because we believe that they may serve as models for the study of fundamental properties of selfcontrolled processes in nature.

In the first section of this paper we recall certain general mathematical properties of (1) and present some general features of stable stationary states obtained from numerical calculations. We then describe a periodic electrical network which has as dynamical equation a discretized version of (1). Next we construct such a network from standard electronic components and show that the stable spatial current and voltage structures obtained experimentally can be understood quantitatively in terms of the discretized version of (1). In the following section we interprete the two dimensional version of the network as the equivalent circuit of a composite material consisting of a linear and a nonlinear layer with s-shaped current density-electric field characteristic. This model with its extentions is used to describe phenomenologically the spatial current and voltage structure and the global current voltage characteristic observed experimentally by Jäger et al. and Baumann et al. [10] in pin-diode like devices and in a gas discharge system [16]. Finally we draw some conclusions from the present work.

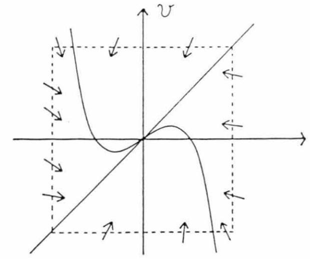

Fig. 1. Phase plane and directions of trajectories of (3) for $\lambda < 1$.

Table 1. Properties of solutions of the uncoupled system (3) for δ, α, $\lambda > 0$.

(v, w)	Parameter range of existence	Parameter range of stability
bounded	unlimited	
$(0, 0)$	unlimited	$\lambda > (1/\delta)$, $\lambda < 1$
$\pm[(\lambda-1)^{1/2}, (\lambda-1)^{1/2}]$	$\lambda > 1$	$\lambda > 1$, $2\lambda + 1/\delta > 3$
limit cycle around $(0, 0)$	$\lambda < 1/\delta$, $\lambda < 1$	$\lambda < 1/\delta$
limit cycle around $\pm[(\lambda-1)^{1/2}, (\lambda-1)^{1/2}]$ and $(0, 0)$ at the same time	$\lambda > 1$, $2\lambda + 1/\delta < 3$	$2\lambda + 1/\delta < 3$

2. General properties of reaction diffusion systems

If we neglect in (1) the coupling by dropping terms containing the Laplace operator we obtain with (2) the two component ordinary differential equation

$$\delta v_{t'} = w - v, \quad \delta, \lambda \geq 0,$$
$$w_{t'} = \lambda w - w^3 - v. \tag{3}$$

It can be seen that (3) is very similar to the van der Pol equation when written in the form

$$w_{t't'} + [(1/\delta) - \lambda + 3w^2] w_{t'} + (1/\delta)[1 - \lambda + w^2] w = 0. \tag{4}$$

From Fig. 1 we conclude that the solutions of (3) and (4) are allways bounded. From (3) and (4) and from linear stability analysis we obtain the stationary states and the ranges of existence and stability as given in Table 1. We note that the trivial stationary state $(0, 0)$ is always a solution and that it is stable for $\lambda < (1/\delta)$ and $\lambda < 1$. It was the discovery of Turing [1] that such a stable homogeneous solution can be destabilized by adding a linear diffusion term and thereby considering spatial extension, and that stable inhomogeneous stationary states may occur instead. In the present work we are interested in the latter. The temporal dependence is only of interest to allow the systems to reach stationary states and to include problems concerning stability.

We now include diffusion and return to (1) and (2). To our knowledge the latter case has been investigated analytically only for $0 < \lambda < 1$ [11–13]. For this case it has been shown that the stable solution $(v, w) = (0, 0)$ of the uncoupled system is diffusion destabelized at least for $\lambda > \sigma^{1/2}(2 - \sigma^{1/2})$. In the particular case of vanishing activator diffusion there are no stable trivial stationary states at all. For $\delta < 1$ the existence of inhomogeneous stable stationary states could be proven under rather general conditions [12, 13]. Also the properties of (1) do not depend sensitively on details of

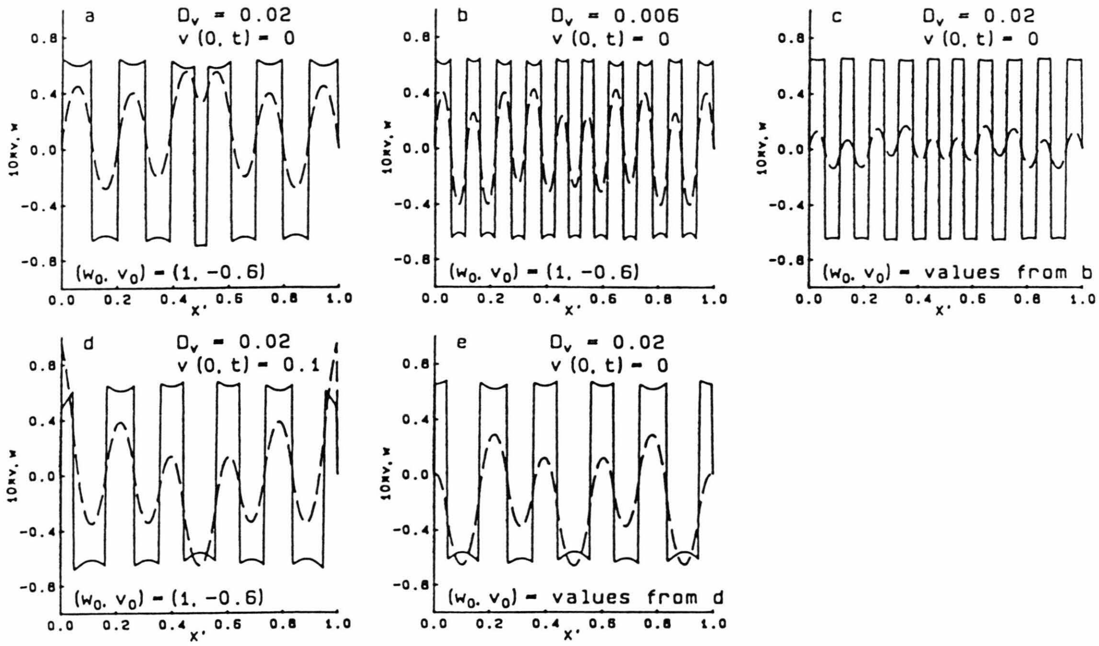

Fig. 2. Stable stationary states of (5) and (2) (v: – – –; w: ——) for $\delta = 7.38$; $\lambda = 0.43$ and $D_w = 0$ using Dirichlet boundary conditions with $v(0,t) = v(1,t) = \text{const.}$ and a discretization length of 1/198.

$f(w)$ if only the general shape of $f(w)$ shown in Fig. 1 is retained [11].

Using hand waving arguments we obtain from (1) and (2) the physical meaning of $\delta, \sigma, \lambda > 0$. Obviously δ is a relative measure for the relaxation time of the inhibitor with respect to the activator. $\delta \gg 1$ means that the autocatalytic increase of the activator is damped efficiently only with large time delay leading to an overshoot of the activator. Large δ therefore favours oscillations, small δ stationary states. σ has the physical meaning of a diffusion constant of the activator measured in units of the inhibitor diffusion. $\sigma \ll 1$ means that the activator distributes badly in space, if in addition λ is large enough the autocatalytic production of activator is locally rather efficient, and due to the good distribution of the inhibitor local accumulation of the activator and therefore inhomogeneous structures are favoured. Also the smaller σ the sharper the spatial structure of the activator. – Last not least the behaviour of the system depends on the boundary condition. Since Dirichlet conditions (predefined value on the boundary) are more stringent than Neumann conditions (predefined flux through the boundary) we conclude that oscillations are favoured by the latter whereas the former favours stationary structures.

In the case that we normalize the space coordinate in (1) to $0 \leq x \leq 1$ we obtain

$$\begin{aligned} \delta v_{t'} &= D_v \Delta v + w - v, \\ w_{t'} &= D_w \Delta w + f(w) - v. \end{aligned} \tag{5}$$

Preluminary numerical investigations of (5) in one-, and to less extent in two-dimensional space in the parameter range where nontrivial stationary states are stable and where we are not too near to instabilities indicate:

1. For suitable parameters the system can have a high degree of multistability, i.e. the reached stationary states depend on the initial conditions (v_0, w_0). A typical situation is demonstrated in Figs. 2a and c.

2. The stationary states can be rather stable with respect to parameter changes: if we choose the stationary states obtained for a given parameter set and $(v_0, w_0) = (-0.6, 1)$ as initial condition of a system where the parameters have been changed by some 100% we observe only minor changes in the new stationary structure (see Figs. 2b and c).

3. A similar behaviour as described for parameter changes under 2. is observed also for changes of boundary conditions (see Figs. 2a, d and e).

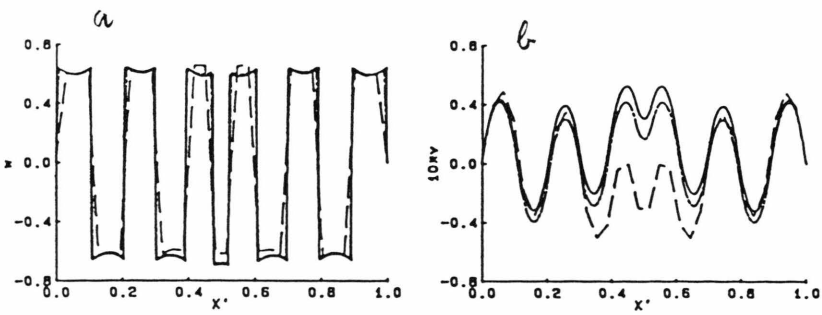

Fig. 3. Stable stationary states of (5) and (2) for parameters used in Fig. 2a and various discretization lengths (1/498:——; 1/98:— — —; 1/31:- - -).

4. Statements 1., 2. and 3. are the weaker the larger is D_w.

5. In general, noise of up to the order of 1% has no critical effect for the formation of the stationary structures for $\lambda < 1$ and $\delta < 1$. However for $\lambda > 1$ noise of less than 1% is able to determine which stationary state is selected.

6. Inhomogeneities up to several per cent in the parameters do not in general affect the stationary structures for $\delta\lambda > 1$ and $D_w = 0$ when Dirichlet boundary conditions are applied; in the case of $\delta\lambda < 1$ parameter fluctuations have to be smaller than 1%.

7. As is expected from physical arguments, the spatial structures smoothen out with increasing diffusion constants in (5). The spatial distribution of the activator tends to infinitely steep slopes in the case that D_w goes to zero.

8. Using about 1/30 of the overall length of the system as discretization length we obtain in general already a good qualitative description of the continuum by the discretized system in so far structures with fundamental wave lengths twice the discretization length are concerned (see Figures 3a, b). The discrepancies around $x' = 0.5$ are due to problems of spatial phase matching.

From the general properties and the physical meaning of (1) and (5) we conclude that these equations may be of considerable interest to describe the temporal and spatial structures of real self controlled systems despite the presence of inevitable inhomogeneities and fluctuations.

3. The network

Since in many cases solutions of (1) can be well approximated by a relatively coarse dicretization it is tentative to check wether a suitable periodic electrical network can be built to simulate solutions of (1) and therefore simulate the structural behaviour of physical systems described by (1). In this chapter we show that we can build a network which is described by a spatially discretized version of (1) with $\sigma = 0$.

In Fig. 4a an element of a periodic array of identical circuits is shown. Thereby the series resistance R_V and the coupling (diffusion) resistance R_D are ordinary linear resistors and L and C', C'' a linear inductance and linear capacities. The only nonlinear element is $R(I)$ which may have the approximate characteristic

$$U = U_0 - \chi'(I - I_0) + \varphi'(I - I_0)^3 = R(I)\,I. \tag{6}$$

As pointed out in the preceeding chapter, the characteristic must not have precisely the form (6). Therefore $R(I)$ can also be realized by a circuit as shown in Fig. 4b with a qualitative characteristic as shown in Figure 4c. The isolated element of Fig. 4a represents a Van der Pol like oscillator with a time constant of the order $(LC)^{1/2}$. $(LC)^{1/2}$ is large in comparison with other time constants in the circuit and therefore determines the time scale of the relaxation processes of the isolated system. The one-dimensional network is realized by coupling many independent oscillators via R_D as indicated in Figure 4a. $(LC)^{1/2}$ turns out to be also the time scale of the coupled system. The whole network is supplied by the boundary voltage $U_L = U_R = \text{const}$ (Dirichlet boundary condition) and by a DC source with internal voltage U_S and internal resistance R_0. We consider first a system with $R_0 = 0$.

If we denote by U_i and I_i the voltage and current as indicated in Fig. 4a we obtain by straight forward application of the Kirchoff rules:

$$\begin{aligned} dU_i/dt &= (1/C)\,[(1/R_D)\,(U_{i+1} - 2\,U_i + U_{i-1}) \\ &\qquad - (1/R_V)\,U_i - I_i + (1/R_V)\,U_V], \\ dI_i/dt &= (1/L)\,[U_i - S(I_i)], \end{aligned} \tag{7}$$

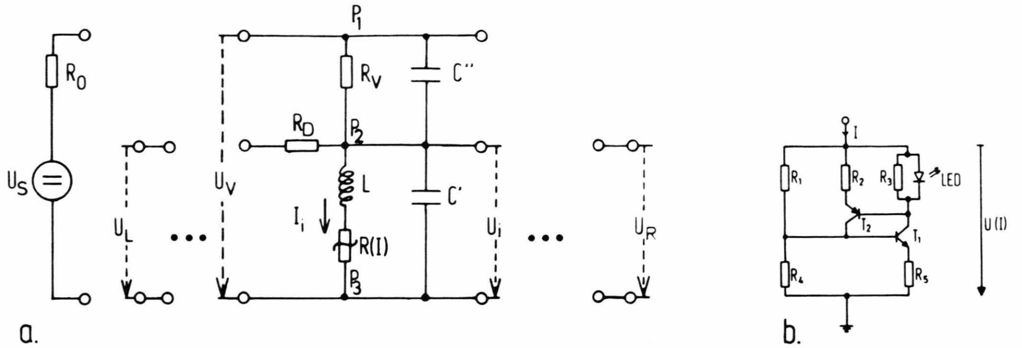

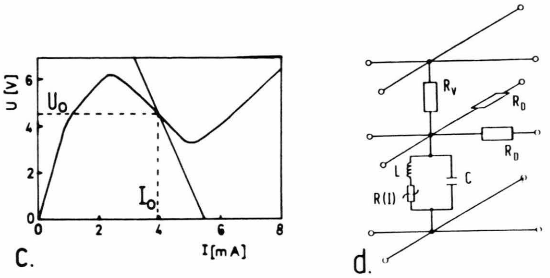

Fig. 4. Element of the electrical network (a), equivalent circuit for the nonlinear resistance $R(I)$ (b), U-I-characteristic of $R(I)$ including the load line of the uncoupled system (c), and two-dimensional electrical network as an equivalent circuit for the linear nonlinear layers structure (d).

$$
\begin{aligned}
C &= C' + C'',\\
S(I_i) &= R(I_i)\, I_i \approx U_0 - \chi'(I_i - I_0)\\
&\quad + \varphi'(I_i - I_0)^3 .
\end{aligned} \tag{8}
$$

We now adjust the bias voltage $U_S = U_V(R_0 = 0)$ so that the load line for $R(I)$ intersects the $R(I)$ characteristic at the inflection point (I_0, U_0) in Figure 4c. Using the transformations

$$
\begin{aligned}
v_i &= (\varphi'/R_V^3)^{1/2}(U_0 - U_i),\\
w_i &= (\varphi'/R_V)^{1/2}(I_i - I_0),\\
t' &= (R_V/L)\,t, \quad I_0 = (U_V - U_0)/R_V,\\
\delta &= R_V^2\, C/L, \quad \lambda = \chi'/R_V
\end{aligned} \tag{9}
$$

we obtain from (7) and (8)

$$
\begin{aligned}
\delta \mathrm{d}v_i/\mathrm{d}t' &= (R_V/R_D)(v_{i+1} - 2\,v_i + v_{i-1}) + w_i - v_i,\\
\mathrm{d}w_i/\mathrm{d}t' &= f(w_i) - v_i \approx \lambda\, w_i - w_i^3 - v_i .
\end{aligned} \tag{10}
$$

Introducing the discretization length $\Delta x = x_i - x_{i-1}$ and the transformation

$$
\begin{aligned}
D_v &= (R_V/R_D)(\Delta x)^2,\\
v_i(t') &= v(x_i, t'),\\
w_i(t') &= w(x_i, t')
\end{aligned} \tag{11}
$$

we obtain from (9) for $(\Delta x) \to 0$

$$
\begin{aligned}
\delta v_{t'} &= D_v \Delta v + w - v,\\
w_{t'} &= f(w) - v .
\end{aligned} \tag{12}
$$

This equation is identical to (1) together with (2) if we put $\sigma = 0$, $x' = D_v^{1/2}\,x$ and $\Delta = \partial^2/\partial x'^2$. Physically $v(x,t)$ and $w(x,t)$ are the normalized one-dimensional voltage and current density.

It is a straight forward matter to extend these considerations to two-dimensional space. For this purpose we build parallel chaines of oscillators as shown in Fig. 4a and connect adjacent chaines at the points P_1 and P_3 directly and the point P_2 via R_D to the neighbouring oscillators. In this way we obtain the two-dimensional network shown in Figure 4d. In analogy to the network equation (7) we obtain the corresponding equation in two-dimensional space

$$
\begin{aligned}
\mathrm{d}U_{i,j}/\mathrm{d}t &= (1/C)\,[(1/R_D)(U_{i+1,j} - 2\,U_{i,j} + U_{i-1,j})\\
&\quad + (1/R_D)(U_{i,j+1} - 2\,U_{i,j} + U_{i,j-1})\\
&\quad - (1/R_V)\,U_{i,j} - I_{i,j} + (1/R_V)\,U_V],\\
\mathrm{d}I_{i,j}/\mathrm{d}t &= (1/L)\,[U_{i,j} - S(I_{i,j})] .
\end{aligned} \tag{13}
$$

Using the transformation (9) by writing i,j instead of i as index we obtain the normalized version of (13):

$$
\begin{aligned}
\delta(\mathrm{d}v_{i,j}/\mathrm{d}t') &= (R_V/R_D)(v_{i+1,j} - 2\,v_{i,j} + v_{i-1,j})\\
&\quad + (R_V/R_D)(v_{i,j+1} - 2\,v_{i,j} + v_{i,j-1})\\
&\quad + w_{i,j} - v_{i,j},\\
\mathrm{d}w_{i,j}/\mathrm{d}t' &= f(w_{i,j}) - v_{i,j} \approx \lambda\, w_{i,j} - w_{i,j}^3 - v_{i,j} .
\end{aligned} \tag{14}
$$

Introducing the discretization lengths $(\Delta x) = (\Delta y)$ and the transformation

$$\begin{aligned} D_v &= (R_V/R_D)(\Delta x)^2, \\ v_{i,j}(t') &= v(x_i, y_i, t'), \\ w_{i,j}(t') &= w(x_i, y_i, t') \end{aligned}$$

we obtain again (12), this time with $\Delta = \partial^2/\partial x^2 + \partial^2/\partial y^2$.

4. Experimental investigation of the electrical network

The electrical network studied experimentally is that shown in Fig. 4a and consists of 33 indentical oscillators with $R_0 = 0$, $U_S = \text{const}$ and U_L, $U_R = \text{const}$. The nonlinear resistance is simulated by the circuit shown in Fig. 4b and the resulting s-shaped I-U characteristic in Figure 4c. The oscillators are coupled by using negative temperature coefficient (NTC-) resistors so that the coupling can be adjusted by changing the temperature. To obtain inhomogeneous stable stationary states we choose parameters corresponding in (10) and (7) to $\lambda > 1/\delta$ and Dirichlet boundary conditions with $U_R = U_L = \text{const}$. Using $L = 1$ mH and $C = 820$ pF we obtain relaxation times of the order $(LC)^{1/2} \approx 10^{-5}$ s. With $R_V = 3000\ \Omega$ we obtain $\delta = 7.4$ and from Fig. 4c $\lambda = 0.43$. R_D can be chosen between 72 and 430 Ω. Switching on U_S and $U_L = U_R$ in much less than 10^{-5} s we obtain the experimental results of Figure 5.

The theoretical calculations on the basis of (7) with standard initial conditions $(U, I) = (0, 0)$ and using the realistic characteristic of Fig. 4c are given also in Figure 5. We find that the agreement between calculation and experiment is very good.

We note that in the experiment and in the calculations of this chapter we have used as characteristic of $R(I)$ the numerical values of Fig. 4c, not the analytical form of the (2) or (6). However, as pointed out in chapter 2 the qualitative behaviour of (1) is not effected much by the detailed shape of $f(w)$, if only $f(w)$ is monotonically decreasing for large $|w|$ and increasing for small $|w|$; $f(w)$ derived from Fig. 4c has this property.

5. The composite material

We now interpret the two dimensional network shown in Fig. 4d as the approximate equivalent circuit of a linear layer L on top of a nonlinear layer N contacted to the outside by metallic films as shown in Figure 6. The linear material is relatively thick so that currents can flow in all directions. The nonlinear layer is thin and currents parallel to the plane may be neglected with respect to currents perpendicular to the plane. Using discretization lengths Δx and Δy for the composite material we put into correspondence each volume element $\Delta x\, \Delta y\,(a + b)$ of the composite material to one oscillator of the above described two-dimensional network. The linear coupling via R_D in the network corresponds formally to diffusion from one volume element to its neighbours. Under these conditions the current in and perpendicular to the interface between L and N of a given volume element (i,j) of the composite material can be identified as $I_{i,j}$ of the equivalent circuit of Fig. 4d under the assumption that contributions due to dielectric displacement currents can be neglected. The potential of the interface of the volume element is interpreted as $U_{i,j}$ in the equivalent circuit.

Choosing $\Delta x = \Delta y$ and denoting by ϱ_L the resistivity of L and by C_s and L_s the capacity and the inductance corresponding to the volume element $\Delta x\, \Delta y\,(a + b)$ we obtain

$$\begin{aligned} R_D &= r\,\varrho_L\,\Delta x/(\Delta y b) &&= r\,\varrho_L/b, \\ R_V &= \varrho_L\,b/(\Delta x\,\Delta y) &&= \varrho_L\,b/(\Delta x)^2, \\ C &= C_s\quad \Delta x\,\Delta y &&= C_s(\Delta x)^2, \\ L &= L_s/(\Delta x\,\Delta y) &&= L_s/(\Delta x)^2, \\ \chi' &= \chi/(\Delta x\,\Delta y) &&= \chi/(\Delta x)^2, \\ \varphi' &= \varphi/((\Delta x)^3(\Delta y)^3) &&= \varphi/(\Delta x)^6, \\ j_{i,j} &= I_{i,j}/(\Delta x\,\Delta y) &&= I_{i,j}/(\Delta x)^2. \end{aligned} \tag{16}$$

In first approximation we get for r the value of 2. In principle r has to be calculated from Maxwell's equations. A deeper analysis of the problem in this direction yields a value of $r \approx 4$ [14]. We choose for further considerations the value of $r = 4$.

Using (13) and (16) and carrying out the transition to the continuum we obtain

$$\begin{aligned} U_t(x,y,t) &= (b/4\,\varrho_L\,C_s)\,\Delta U(x,y,t) \\ &\quad - (1/\varrho_L\,C_s\,b)\,U(x,y,t) - (1/C_s)\,j(x,y,t) \\ &\quad + (1/\varrho_L\,C_s\,b)\,U_V, \end{aligned} \tag{17}$$

$$j_t(x,y,t) = (1/L_s)\,[U(x,y,t) - s(j(x,y,t))],$$

$$s(j) = U_0 - \chi(j(x,y,t) - j_0) + \varphi(j(x,y,t) - j_0)^3, \tag{18}$$

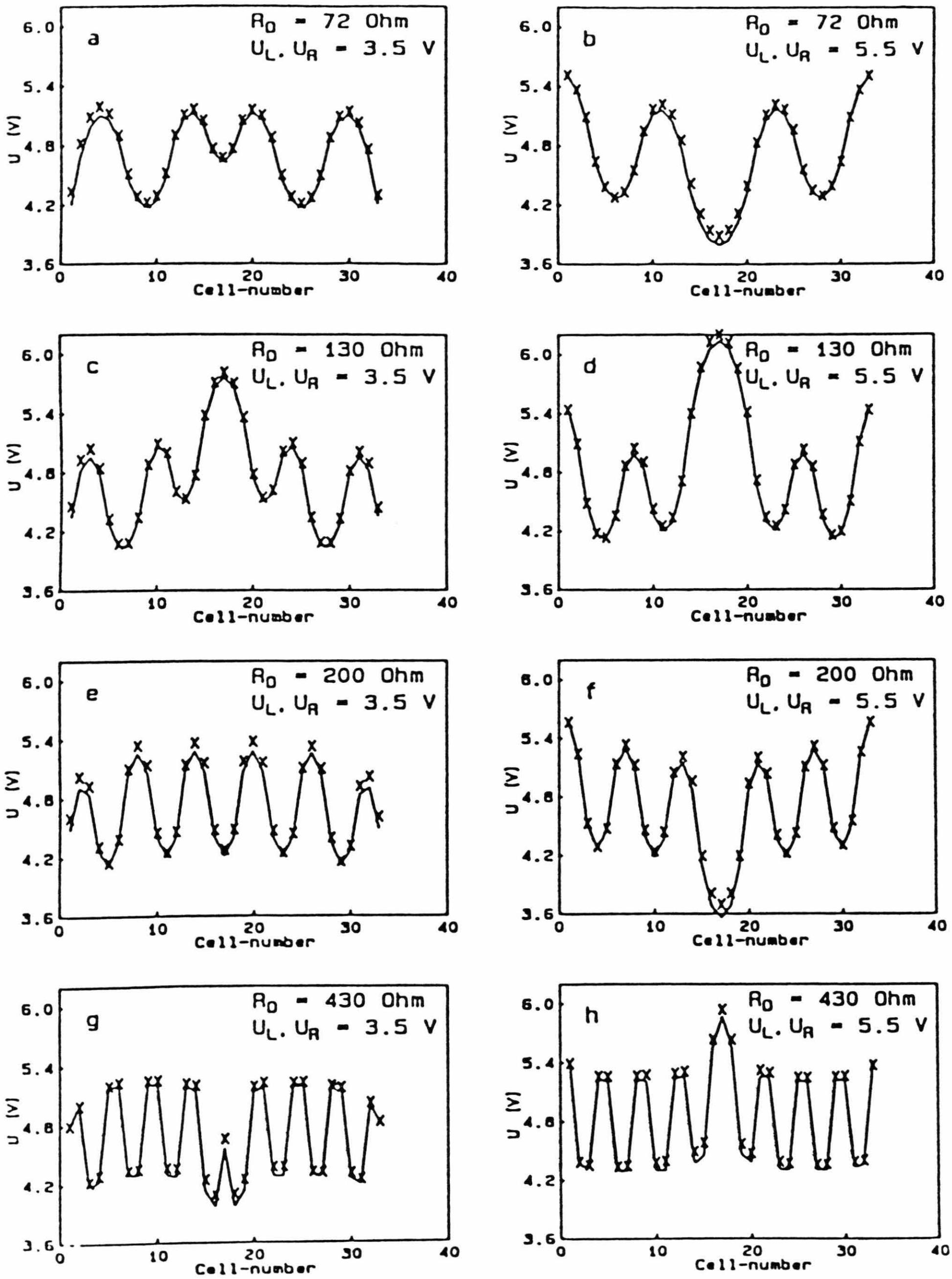

Fig. 5. Experimental points and calculated lines for the voltage distribution of an electrical network consisting of 33 coupled oszillators according to Fig. 4 with $R_0 = 0$, $L = 1$ mH, $C = 820$ pF, $R_V = 3000\ \Omega$ and R_D and $U_L = U_R$ as indicated in the figure.

$s(j)$ is the U-j-characteristic of the nonlinear material with the inflection point (j_0, U_0). Also U_S is choosen such that in the homogeneous situation the load line interects the nonlinear characteristic at (j_0, U_0). Equation (16) can easily be transformed into (12) and (1) with $\sigma = 0$.

Equation (17) describes the current and voltage distribution in the interface of our composite material. Though writing the U-j-characteristic of our device as a polynomial of third order we could argue, as we have done at the end of Chapt. 4, that we can take other forms if only the general shape is retained as described in Chapter 2. We also note that due to the fact that C' is parallel to L and $R(I)$ and C'' parallel to R_V in Fig. 4d, C contains the voltage relaxation of the linear and nonlinear layer.

Equation (17) does contain a "voltage diffusion" in the interface of the composite material but "current diffusion" is not taken into account. However charge carrier diffusion is an essential property of many conducting materials. For the sake of a more general applicability of our model we therefore add a term $D\,\Delta j(x, y, t)$ to the second part of (17).

Also we consider a variable source voltage $U_S + \Delta U$ and the case $R_0 \neq 0$. The former is of interest to obtain the overall characteristic of our device. U_S is again the external voltage that would lead in the homogeneous situation to an intersection of the load line with the nonlinear characteristic at the inflection point for $\Delta U = 0$. $R_0 \neq 0$ may be necessary in many experimental situations in order to limit the total current to prevent destruction of the device. The final integro-differential equation describing the current density j and the potential U in the interface of Fig. 6 then reads

$$\begin{aligned} U_t(x, y, t) &= (b/4\varrho_L C_s)\Delta U(x, y, t) \\ &\quad - (1/\varrho_L C_s b)\, U(x, y, t) - (1/C_s) j(x, y, t) \\ &\quad + (1/\varrho_L C_s b)\, U_V, \\ j_t(x, y, t) &= D\,\Delta j(x, y, t) \\ &\quad + (1/L_s)[U(x, y, t) - s(j(x, y, t))], \\ U_V &= U_S + \Delta U - R_0 \int_0^l \int_0^d j(x, y, t)\,dx\,dy \\ &= U_S + \Delta U - R_0 I. \end{aligned} \tag{19}$$

In this equation we have neglected the dielectric displacement current with respect to j. – The problem is completely defined if we give the boundary conditions. For the device shown in Fig. 6 we believe that Neumann conditions with zero flux normal to the boundary are reasonable.

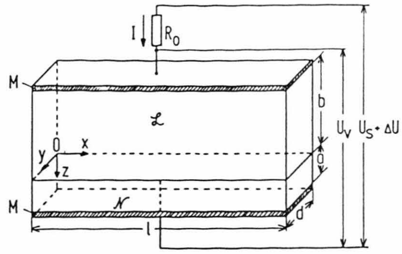

Fig. 6. Layer structure of the composite material: L = linear material, N = high ohmic nonlinear material, M = metallic contacts.

Using the transformation

$$\begin{aligned} v &= (\varphi/(\varrho_L b)^3)^{1/2}(U_0 - U), \\ w &= (\varphi/\varrho_L b)^{1/2} \quad (j - j_0); \\ t' &= t\,\varrho_L b/L_s, \\ x' &= (2/b)\,x, & x_0' &= 2l/b, \\ y' &= (2/b)\,y, & y_0' &= 2d/b; \\ \sigma &= 4L_s D/\varrho_L b^3, & \lambda &= \chi/\varrho_L b, \\ \delta &= C_s \varrho_L^2 b^2/L_s, \\ \varkappa_1 &= (\varphi/(\varrho_L b)^3)^{1/2}\Delta U, \\ \varkappa_2 &= R_0 b/4\varrho_L; \\ j_0 &= (1/\varrho_L b)\left(U_S - U_0 - R_0 \int_0^l \int_0^d j_0\,dx\,dy\right) \end{aligned} \tag{20}$$

we obtain

$$\begin{aligned} \delta v_t' &= \Delta' v + w - v - T, \\ w_t' &= \sigma \Delta' w + f(w) - v, \end{aligned} \tag{21}$$

$$T = \varkappa_1 - \varkappa_2 \int_0^{x_0'} \int_0^{y_0'} w\,dx'\,dy', \tag{22}$$

$$f(w) = \lambda w - w^3. \tag{23}$$

Equation (21) together with (22) is an integro-differential equation and cannot be transformed into (1). To our knowledge this type of equation has not been investigated by analytical tools so far. However some physical insight may be obtained from the network analogon. Choosing the case $R_0 = 0$ we see from (21)–(23) that in Fig. 1 $\Delta U \neq 0$ results in a parallel displacement of the load line (straight line). For $\lambda < 1$ the load line in Fig. 1 intersects the characteristic of the nonlinear resistor always in one point. Consequently we expect off hand that if a stable stationary state exists at $\Delta U = 0$ it will also exist somewhere around $\Delta U \neq 0$, and there will be a continuous dependence of the total current on the supply voltage offset leading in (19) to a continuous J-U_V-characteristic of the device. For $\lambda > 1$ there is one intersection point for $\Delta U \ll 0$. In addition a pair of two points appear at an other place of the nonlinear characteristic for values of ΔU around 0. For increasing ΔU the first point coalesces with one of the others and finally disappears. This means that the I vs. U curve exhibits a jump, and also hysterese effects occur. Allowing for $R_0 \neq 0$, the situation is even more interesting for $\lambda > 1$. There may be many jumps and the system can jump back resulting in a multivalued curve even if we monotonically increase ΔU (cf. also Chapt. 6 and Figure 9).

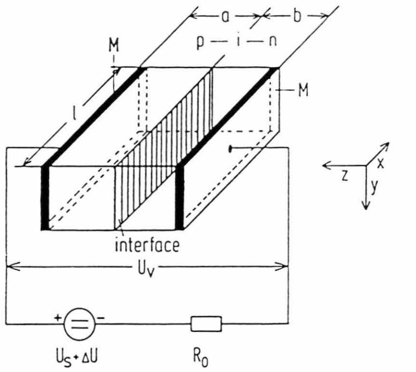

Fig. 7. Pin-diode like device with the hypothetical layer somewhere in the p-i-region.

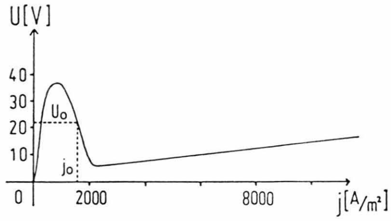

Fig. 8. Characteristic of the nonlinear material N used for the calculation of the characteristic of Fig. 9 and the current density distribution of Figure 10.

6. Numerical results for the composite material

We now want to investigate numerically an example of a linear-nonlinear layer structure as shown in Fig. 6 by calculating the spatial stationary distribution of U and j in the interface of Fig. 6 and also the J-U_V-characteristic. To be specific we need the numerical values of the parameters and the s-shaped characteristic of the nonlinear part of the device. In the choice of these values it is desirable to be as near as possible to situations studied experimentally.

Unfortunately, to our knowledge there are no detailed investigations of the stable spatial structures of a device as shown in Figure 6. However there are interesting measurements on current and potential structures in semiconductor pin diode like devices performed by Jäger et al. and Baumann et al. [10]. We believe that under favorable conditions the currents and potentials in a fictive plane of these devices can be described by our model. We therefore estimate the numerical values needed for our calculations from typical values of semiconductor devices investigated in this work.

A typical pin diode like strukture is shown in Figure 7. The device is made of n-type Si compensated with Au and finally doped at the fronts with P and B to obtain the n- and p-regions, respectively. An additional Al-layer on top of the fronts serves as a low ohmic contact. Such devices exhibit s-shaped current density-electric field characteristics [15].

Under special conditions there is a steep potential drop somewhere near the p region and a flat drop in the rest of the i- and n-regions. This relatively thin layer is interpreted as the high ohmic nonlinear layer and the rest as the thick low ohmic layer of Figure 6. The steeper the potential drop in the p-i-region and the flatter the drop in the i-n-region the better the device of Fig. 7 is modelled by the layer structure of Figure 6. On such devices Jäger et al. and Baumann et al. [10] have made qualitative measurements of the global J-U_V-characteristic and of spatial current and potential structures.

We are now ready to estimate typical values for the parameters and the U-j-characteristic of N necessary to solve (19) to obtain stationary voltage and current distributions and the overall I-U_V-characteristic of the device. Referring to [10] and [15] we take:

$$\begin{aligned}
&a = 1.2 \cdot 10^{-4}\,\mathrm{m}, \quad b = 3.8 \cdot 10^{-4}\,\mathrm{m}, \quad \varrho_L = 10\,\Omega\mathrm{m}, \\
&l = 5.6 \cdot 10^{-3}\,\mathrm{m}, \quad d = 2.0 \cdot 10^{-4}\,\mathrm{m}, \quad R_0 = 37696\,\Omega, \\
&U = U(j) \quad \text{from Fig. 8}, \qquad (23) \\
&C_s = C_s' + C_s'' = (\varepsilon_L/b + \varepsilon_N/a) \approx 10^{-6}\,\mathrm{As/Vm^2}, \\
&L_s \approx \tau_N\, as(j_0)/aj_0 = \tau_N\, s(j_0)/j_0 \approx 1.4 \cdot 10^{-9}\,\mathrm{Vsm^2/A}, \\
&D \approx 0.95 \cdot 10^{-2}\,\mathrm{m^2/s}.
\end{aligned}$$

C_s is obtained from the dielectric constants ε_L and ε_N and considering C' and C'' as capacities of the condensators represented by the linear and nonlinear layer. L_s is interpreted as being due to the charge carrier relaxation time τ_N of the nonlinear material. According to the equivalent circuits of Figs. 4a, d, L_s can be estimated from τ_N and the resistivity of the nonlinear material. For τ_N we estimate a value 10^{-7} s and for the resistivity the value at the inflection point. We believe that the estimate of τ_N and C_s is roughly of the correct order of magnitude. From (20) we therefore expect $\delta < 1$. From what has been said in Sect. 2, stability of inhomogeneous stable stationary states is to be expected. This stability is supported by the numerical calculations. Under the condition $\delta < 1$ the stability of the stationary states does not depend on τ_N. – D is related to the charge carrier diffusion and is estimated to be $D = 10^{-2}$ m^2/s. According to (20) this corresponds to $\sigma = 0.1$.

The numerical calculations have been performed with no flux boundary conditions and by starting with zero external voltage ($\Delta U = U_S$), which gives the trivial solution ($U(x, y, t) = 0$, $j(x, y, t) = 0$). We then proceed in steps of increasing ΔU, calculating $U(x, y, t)$ and $j(x, y, t)$ for large time and the corresponding points in the I-U_V-characteristic, each time using as initial condition the stationary voltage and current distribution for the preceeding value of ΔU. The stationary stable states resulting from these calculations are the full lines in the I-U-characteristic of Figure 9. Examples for the stable spatial distributions of the current density j for such states are given in Figure 10. The letters indicate the correspondence between the branches of the characteristic and the spatial structures of the current density distribution.

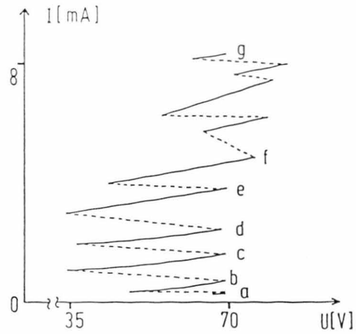

Fig. 9. Calculated total current I through the device in Fig. 6 as a function of voltage U_V for increasing $U_S + \Delta U$. a–g indicate the points for which the spatial voltage and current distributions are given in Figures 10a–g.

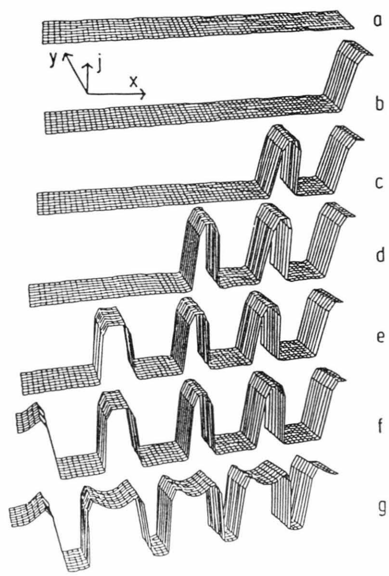

Fig. 10. Calculated current density distribution of the device of Fig. 6 for parameters as given in (23). a–g correspond to the branches a–g in Figure 9.

From Figs. 9 and 10 we conclude that the main qualitative features observed in the experiments by Jäger et al. and Baumann et al. [10] on pin-diode like devices can be described in the framework of the present model:

– For very low and, as can be shown, for very high external supply voltages stable homogeneous stationary states are obtained. Physically this is evident from the shape of the j-U-characteristic of the nonlinear material.

– The model yields stable stationary inhomogeneous states as observed in the space resolving potential and current measurements.

– Being not too near to one another the inhomogeneous stable states can be interpreted in terms of well defined current filaments. In addition all filaments have the same maximum value within one structure and within 20% the same width.

– The model as well as the experiment show discontinuities in the I-U_V-characteristic of our device even if the external supply voltage is monotonically increased. The characteristic can therefore consist of several successively appearing disconnected branches where in general after the jump the continuation of the characteristic at higher I takes place at lower voltages compared to the highest value of the foregoing branch.

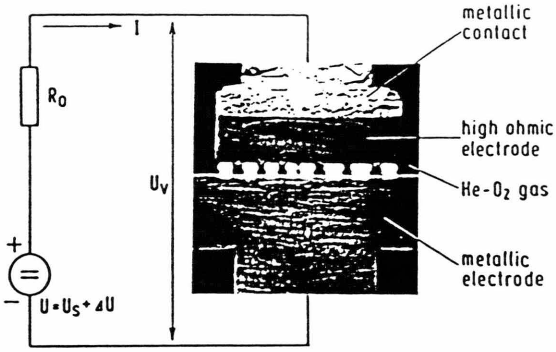

Fig. 11. Experimental set up of the gas discharge system.

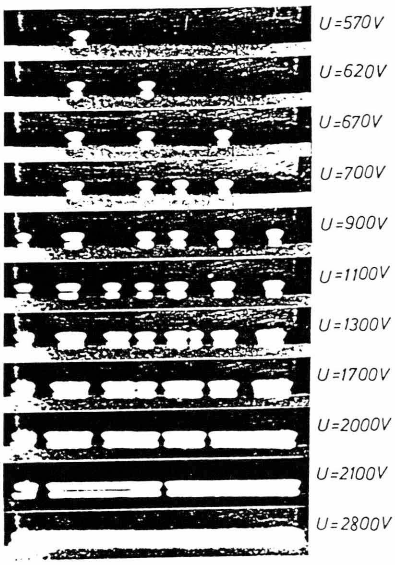

Fig. 12. Photos of the filament structure of the gas discharge system for increasing voltage $U = U_S + \Delta U$.

– The change of the number of filaments results in discontinuous jumps in the I-U_V-characteristic. However, theory indicates that this can be the case also due to discontinuous filament broadening. This effect remains to be investigated experimentally.

All calculations have been done with 1% amplitude limited noise and the condition that the load line intersects the nonlinear characteristic 3 times ($\lambda > 1$). It turns out that the I-U_V-characteristic is very sensitive to noise, thus e.g. increasing the noise can lead to the disappearence of one or several branches in the I-U_V-characteristic. This is an indication that certain

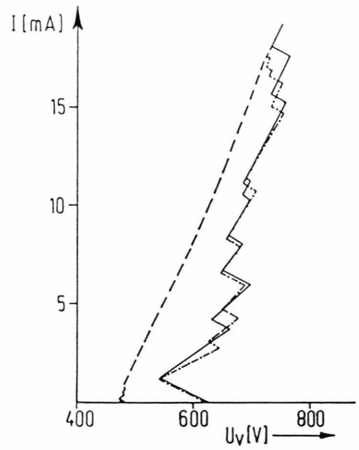

Fig. 13. I-U-characteristic ($U = U_S + \Delta U$) for the device of Fig. 11 measured in a quasistationary manner (—— increasing U, – – – decreasing U, – · – · – repetition with increasing U).

stable branches have a very small attractor. Therefore a quantitative comparison between calculation and experiment has to include a careful analysis of noise.

Another realization of the device of Fig. 6 that should be describable qualitatively by (19) and (21) is a gas discharge system as shown in Figure 11. Indeed investigations of Radehaus et al. [16] give the filament structure and typical I-U-characteristic as shown in Figs. 12 and 13. The behaviour of the system is very similar to that of the pin-diode like devices and the results obtained by solving (19).

7. Discussion and Conclusions

In the present paper we describe a simple two-component nonlinear activator inhibitor reaction diffusion equation, (1), and lay emphasis on the possible spatial structures. We demonstrate that this equation has many mathematical properties allowing for a description of real physical systems with their inevitable fluctuations and inhomogeneities. In particular, with suitably choosen parameters the equation has stable stationary inhomogeneous states with a reasonably large range of attraction. The richness of these structures observed when the parameters are changed is very large. Thus physical systems described by the equation should have many interesting structure forming properties. We only mention the solitary like behaviour of current filaments which allows to construct qualitatively the spatial structure from filaments considered as fundamental building blocks. Also a high degree of multistability is observed, and the particular state depends on the way one runs into the stationary state. Simulations show that in many cases solutions do not depend strongly on fluctuations of the variables or inhomogeneities of parameters. We note further that modifications in the nonlinearity of our system do not effect much the fundamental properties if only the general shape of the nonlinearity is retained. Finally, it is interesting to see that in numerical calculations the discretization of the problem can be rather course in many cases without destroying the main structural properties of the continuum equation. All these properties encourage to look for real physical systems described by our reaction diffusion equation and also to investigate discrete physical systems.

We further demonstrate that an analogue network consisting of simple electronic components can be built which is described by the discretized version of (1). We find excellent agreement between theory and experiment. Since our system is heavily nonlinear this is not a trivial statement. We conclude therefore that by constructing the network we have realized a physical object with many interesting properties already observed or still to be discovered. At the same time we may consider the network as a simulator for other physical systems also described by (1) with $\sigma = 0$, thus considering our network as a fast analogue computer. However, much further work has to be done to clarify completely the latter statement.

Considering a two dimensional electrical network described by the discretized version of (1) as an equivalent circuit one is lead to a solid state composite layer structure with a low ohmic linear material on top of a high ohmic nonlinear material. We can show that the current density vertical to the interface of the two materials and the potential in the interface can be described by an equation closely related to (1). This model is entirely phenomenological and the main input is the S-shaped characteristic, the relaxation constant and the diffusion constant of the nonlinear material. However, to scope with experimental situations often present when measuring electrical properties of nonlinear devices we have to extend (1) to an integro-differential equation. Fortunately many qualitative features of the behaviour of a system described by this equation can be derived from (1) so that the relation between (1) and the integro-differential equation is indeed very close.

Applying our model to pin-diode like devices and using realistic parameters for a numerical calculation we see that the main qualitative features of the global characteristic and the spatial structures observed in the experiment are well reproduced. In particular the solitary like behaviour of the spatial current density structure where qualitatively current filaments can be considered as fundamental elements of the structure are of interest. Creation or anihilation of these filaments leads to discontinuous transitions. This can occur when parameters of the systems destabilize certain structures when changed monotonically. Our model shows that discontinuous changes in the filament width can lead to discontinuities of the system also. – As indicated, these ideas can be transferred to gas discharge systems too.

In summary we may state that a model is proposed that allows for a description of spatial pattern formation of various physical systems. For electrical networks this model works quantitatively. For pin-diode like devices and gas discharge systems it seems to be applicable at least qualitatively. We have evidence that it describes also spatial structures in certain thyristor like devices. We believe that physical systems described by the type of equation treated in this article should be of great interest for fundamental investigations of pattern formation in nature*.

Acknowledgement

We are grateful to Prof. Dr. D. Jäger and Dipl.-Phys. H. Baumann for stimulating discussions and to R. Dohmen and F. J. Niedernostheide for help in doing some calculations.

* After finishing this article we became aware of the work of F. J. Elmer (unpublished so far) discussing analytically some aspects of Equations (21)–(23).

[1] A. M. Turing, Phil. Trans. Roy. Soc. **B 237,** 37 (1952).
[2] J. Smoller, Shock Waves and Reaction-Diffusion Equations, Springer-Verlag Berlin 1984.
[3] P. Fife, Mathematical Aspects of Reacting and Diffusing Systems, Springer Lecture Notes in Biomath. **1979,** p. 28.
[4] F. Rothe, Global Solution of Reaction-Diffusion Systems, Springer Lecture Notes in Math., **1984,** 1072.
[5] J. Murray, Lectures on Nonlinear Differential Equation Models in Biology, Claredon Press, Oxford 1977.
[6] S. E. Trullinger, V. E. Zakharov, and V. L. Pokrovsky, Solitons, North-Holland, Amsterdam 1986.
[7] G. Nicolis and I. Prigogine, Self-Organisation in Nonequilibrium Systems, John Wiley, New York 1977. – H. Haken, Advanced Synergetics, Springer-Verlag Berlin 1983. – A. Gierer, Prog. Biophys. Molec. Biol. **37,** 1 (1981). – F. Schlögl, Z. Physik **253,** 147 (1972).
[8] E. Schöll, Z. Physik B-Condensed Matter **62,** 245 (1986).
[9] B. S. Kerner and V. V. Osipov, Sov. Phys. JETP **47,** 874 (1978).
[10] D. Jäger, H. Baumann, and R. Symancyk, Phys. Lett. **A 117,** 141 (1986). – H. Baumann, Th. Pioch, H. Dahmen, and D. Jäger, Scanning Electron Microscopy/1986/**II,** 441 (1986).
[11] K. Maginu, Math. Biosciences **27,** 17 (1975).
[12] F. Rothe, J. Math. Biology **7,** 375 (1979).
[13] F. Rothe, Nonlinear Analysis, Theory, Methods, and Applications **5,** 487 (1981).
[14] C. Radehaus, Thesis, University of Münster 1987.
[15] J. Dudeck and R. Kassing, J. Appl. Phys. **48,** 4786 (1977).
[16] C. Radehaus, T. Dirksmeyer, H. Willebrand, and H.-G. Purwins, Phys. Letters A **125,** 92 (1987).